THE JOURNAL OF PHYSICAL CHEMISTRY B

Article

pubs.acs.org/JPCB

Label-Free Detection of Prion Protein with Its DNA Aptamer through the Formation of T-Hg^{2+}-T Configuration

Sai Jin Xiao,[†,‡] Ping Ping Hu,[§] Geng Fu Xiao,[⊥] Yi Wang,[†] Yue Liu,[¶] and Cheng Zhi Huang*[,†,¶]

[†]Education Ministry Key Laboratory on Luminescence and Real-Time Analysis, College of Chemistry and Chemical Engineering, Southwest University, Chongqing 400715, P. R. China

[‡]Jiangxi Key Laboratory of Mass Spectrometry and Instrumentation, Department of Applied Chemistry, East China Institute of Technology, Nanchang 330013, P. R. China

[§]College of Life Sciences, Southwest University, Chongqing 400715, P. R. China

[⊥]State Key Laboratory of Virology, Wuhan Institute of Virology, Chinese Academy of Sciences, Wuhan 430071, P. R. China

[¶]College of Pharmaceutical Sciences, Southwest University, Chongqing 400715, P. R. China

ABSTRACT: Though rapid tests were developed for mass screening of prion diseases in the last century, bovine spongiform encephalopathy (BSE) was still epidemic in some European countries. The main reason is that the sensitivity of such tests is insufficient for detecting animals that are incubating with prion diseases at the presymptomatic stage. Driven by this, in this contribution, we developed a novel sensitive label-free method taking advantage of DNA aptamer for prion proteins (PrP) detection through the formation of T-Hg^{2+}-T configuration. In the presence of Hg^{2+} ions, double-strand structures formed due to the strong binding affinity of Hg^{2+} ions to the T bases of DNA aptamer, which dramatically enhanced the fluorescence of Syber Green I, a double-strand indicator. With the addition of prion protein, however, the specific interaction between prion protein and its aptamer forced the destruction of the double-strand structures, and thus the fluorescence of Syber Green I decreased. It was found that there is a linear relationship between the decreased fluorescence intensities and prion protein concentration ranging from 13.0 to 156.0 nmol/L. Compared with other methods, the method presented here holds the advantages of being label-free, rapid, highly sensitive, and selective, which shows great promise for clinical application.

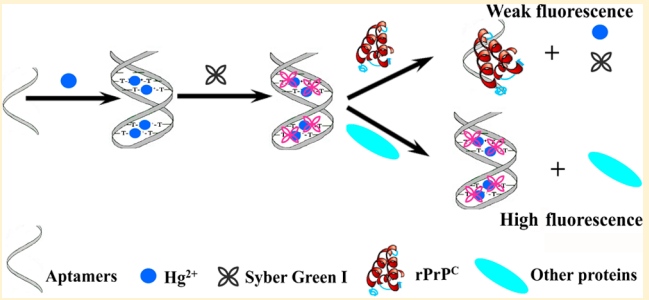

1. INTRODUCTION

Post-mortem rapid tests, which have to process numerous samples in just a few hours, were developed for the huge epidemic bovine spongiform encephalopathy (BSE) in Europe in the last century.[1,2] With the implementation of such tests, more than 2500 infected animals were detected compared with those detected by negative inspection from 1996 to 2001.[2] However, BSE is still epidemic in some European countries as the sensitivity of such tests is insufficient for detecting animals that are infected by prion diseases at the presymptomatic stage; thus, they cannot be distinguished and still enter the food chain. Until recently, none of the current methods was suitable for presymptomatic diagnosis.

Aptamers, which possess the advantages of high affinity and selectivity, excellent stability, and easy reproducibility and manipulation, and are nontoxic and nonimmune, have been widely applied in protein detecting,[3−6] cancer diagnosis,[7−9] cell imaging,[10,11] virus tracking,[10,12] etc. For the purpose of disease diagnosis, DNA aptamers are superior to RNA aptamers (except for 2′-modified RNA aptamers) owing to their higher resistance to nuclease,[13] which might be critical to disease diagnosis in living organisms when aptamers are incubating with enzyme-rich materials such as body fluids and tissue homogenates.[13] Aptamers against prion protein (PrP) were selected taking the advantage of the known capacity of PrP to bind with nucleic acids.[13−18] For example, Bibby et al. found that a trivalent pool of DNA aptamers could bind with guanidinium-denatured PrP^{Res},[18] motivating researchers develop highly sensitive and selective PrP^{Res} detection system similar to the conformation-dependent immunoassay. Along this line, we developed a new dual-aptamer strategy by using DNA aptamers for sensitive discrimination and detection of prion disease associated isoform (PrP^{Res}) in serum and brain homogenate.[19] The method is highly sensitive and specific while the immobilization and modification of DNA aptamers to nanoparticles might reduce the affinity of aptamers to PrP^{Res} and also is laborious and cost-consuming. In order to overcome these shortcomings, herein we further developed a label-free method for sensitive prion protein detection using its DNA aptamer through the formation of T-Hg^{2+}-T configuration.

Received: September 15, 2011
Revised: July 18, 2012
Published: July 23, 2012

dx.doi.org/10.1021/jp302522b | J. Phys. Chem. B 2012, 116, 9565−9569

Scheme 1 displays the operation route of our present label-free strategy. Our work started from the selection of T-rich

Scheme 1. Schematic Representation of Label-Free Detection of Recombinant Prion Protein ($rPrP^C$) Based on Hg^{2+} and DNA Aptamer

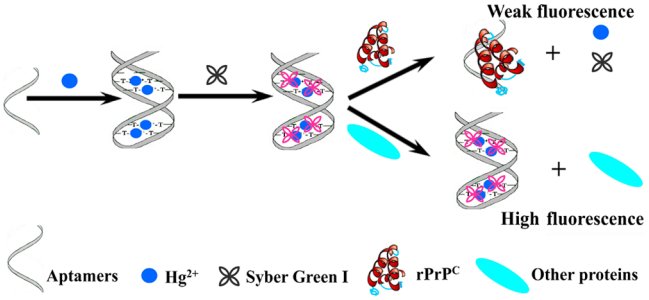

DNA aptamer with the sequence of 5′-GTT TTG TTA CAG TTC GTT TCT TTT CCC TGT CTT GTT TTG TTG TCT-3′, which can easily form the T-Hg^{2+}-T configuration in the presence of Hg^{2+}.[20−23] The DNA aptamer of prion protein (PrP) was commercially synthesized by Invitrogen (Germany), and recombinant cellular PrP ($rPrP^C$) was isolated and purified according to ref 24. In the presence of Hg^{2+} ions, the specific and strong binding affinity of Hg^{2+} ions to thymine bases induced the formation of T-Hg^{2+}-T base pairs. Thus, a double-strand structure was readily formed with inter- or intra-DNA aptamer resulting in a significant fluorescence enhancement of the double-strand specific dye Syber Green I. With the addition of $rPrP^C$, however, the double-strand structure was destructed by the specific interaction of DNA aptamer and $rPrP^C$ with the result of decreasing the enhanced fluorescence of Syber Green I. Compared with previous reports, the current strategy holds three advantages. First, our proposal presents a label-free strategy, avoiding any modification or immobilization of DNA aptamer, and thus the binding affinity of DNA aptamer can be completely maintained. Second, the current method is very fast and easily operated, and everyone, even one who is not a professional, is capable of achieving the detction. Third, the label-free method developed here simplifies the detection steps and reduces the cost.

2. EXPERIMENTAL SECTION

2.1. Apparatus. Fluorescence spectra were measured with a Hitachi F-2500 fluorescence spectrophotometer. The circular dichroism (CD) spectra were obtained by a J-810 spectropolarimeter (JASCO Co., Japan).

2.2. Reagents. DNA aptamer, 5′-GTT TTG TTA CAG TTC GTT TCT TTT CCC TGT CTT GTT TTG TTG TCT-3′, was selected by Bibby[18] and synthesized by Invitrogen (Germany) without further purification. Gdn-HCl was purchased from Genview (USA). Ultrapure water (18.2 MΩ, LD-50G-E Lidi Ultra Pure Waters System, Chongqing, China) was used throughout. Human serum albumin (HSA) and bovine serum albumin (BSA) were purchased from Shanghai Biotech (Shanghai, China). Lysozyme, thrombin, snailase, IgG, and fibrin were purchased from Sigma (USA). Other commercial reagents such as sodium chloride and nickel chloride were analytical reagents without further purification.

2.3. Purification of Recombinant Prion Proteins ($rPrP^C$) and the Conversion of $rPrP^C$ to the Disease-Associated Isoform (PrP^{Res}). The isolation and purification of $rPrP^C$ were done according to ref 24. Briefly, 50 μg/mL isopropyl-D-thiogalactopyranoside (Sigma, USA) was used to induce the fresh overnight culture, and the cell was harvested by centrifugation after 6 h and sonicated in lysis buffer (50 mmol/L NaH_2PO_4, 300 mmol/L NaCl, and 10 mmol/L imidazole, pH 8.0). Then the resulting solution was denatured in 6 mol/L guanidine hydrochloride (Gdn-HCl) overnight and purified by nickel−nitrilotriacetic acid agarose resin (Invitrogen, Germany). Finally, the purified prion protein was analyzed by SDS−polyacrylamide gel electrophoresis and CD spectra, and the concentration was determined with the Bradford Protein Assay Kit (TianGen, Beijing).

The conversion of $rPrP^C$ to PrP^{Res} was done according to the ref 25. Briefly, 22 μmol/L PrP^C was incubated at 37 °C with 3 mol/L urea, 1 mol/L Gdn-HCl, and 150 mmol/L NaCl at pH 4.0 in 20 mmol/L sodium acetate buffer for 48 h, and then dialyzed with sodium acetate buffer.

2.4. General Procedures. 40 μL of 1.0×10^{-7} mol/L DNA aptamer, certain concentrations of Hg^{2+} ions, and 40 μL of Syber Green I were incubated for 30 min in the presence of 20 mmol/L PB buffer (pH 7.4) and 0.2 mol/L NaCl. The fluorescence of Apt−Hg^{2+} complexes could be measured with the excitation at 490 nm and emission at 529 nm, which is predominant from the Syber Green I emission. For the detection of $rPrP^C$ or PrP^{Res}, certain concentrations of $rPrP^C$ or PrP^{Res} were added into Apt−Hg^{2+} complexes and incubated for 30 min more; the fluorescence was measured with the excitation at 490 nm and emission at 529 nm, which is predominant from the Syber Green I emission.

3. RESULTS AND DISCUSSION

3.1. Fluorescence of DNA Aptamer−Hg^{2+} Ion Complexes. The DNA aptamer of prion protein selected by Bibby and co-workers is rich with T bases, and Figure 1 shows the interaction of DNA aptamer and Hg^{2+} ions as indicated by Syber Green I, the fluorescence intercalated dye. In the presence of DNA aptamer alone, the fluorescence of Syber Green I was relatively weak. With the addition of Hg^{2+}, however, sequential increases of the fluorescence emission

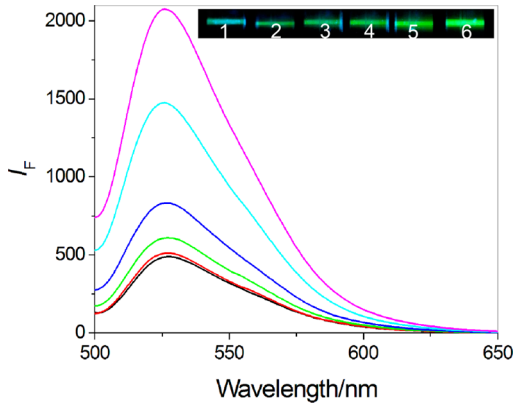

Figure 1. Fluorescence spectra of DNA aptamer incubating with Hg^{2+} ions. The inset pictures are photographed directly from the side window of the F-2500 spectrofluorometer when excited at 490 nm, showing that the fluorescence emission enhances with increase in Hg^{2+} ions. 10 nmol/L DNA aptamer was incubated with 0, 0.03, 0.15, 0.3, 3, and 30 × 10^{-6} mol/L Hg^{2+} ions (from bottom to top of the fluorescence spectra and from left to right of inset image) in the presence of 20 mmol/L PB buffer (pH 7.4) and 0.2 mol/L NaCl.

dx.doi.org/10.1021/jp302522b | J. Phys. Chem. B 2012, 116, 9565−9569

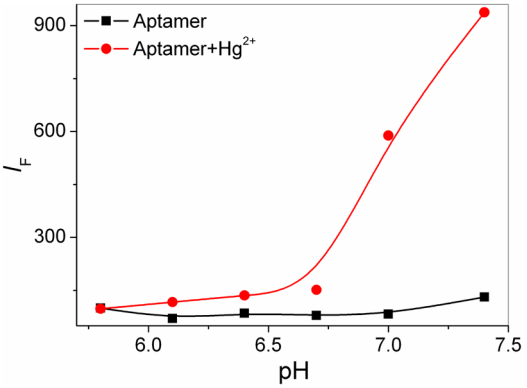

Figure 2. Fluorescence emission of DNA aptamer incubating with Hg^{2+} ions at different pH. 10 nmol/L DNA aptamer was incubated with 3 μmol/L Hg^{2+} ions in the presence of 20 mmol/L PB buffer and 0.2 mol/L NaCl.

characterized at 529 nm could be observed when DNA aptamer was incubated together with increasing concentration of Hg^{2+} ions. The strong fluorescence emission could also be visualized directly through the digital pictures (inset in Figure 1). The blue color of photograph 1 was owing to the Rayleigh scattering signals of DNA aptamer, and the green color of the emission became more obvious with increasing Hg^{2+} ion concentrations (photographs 2–6). All the results mentioned above indicate that double-strand structures formed because of the specific and strong binding affinity of Hg^{2+} ions to T bases.

3.2. Influence of pH on the Interaction between DNA Aptamer and Hg^{2+} Ions. During the experiment, it was found that pH obviously affected the formation of DNA aptamer–Hg^{2+} ion complexes, as shown in Figure 2. From pH 5.8 to 7.4, the fluorescence intensities of aptamer alone were relative weak, and no obvious fluorescence enhancement was observed when DNA aptamer were incubated with Hg^{2+} at pH 5.8, indicating that the T-Hg^{2+}-T configuration was not exiting. From pH 6.1, however, the fluorescence intensities increased gradually, especially when pH values were higher than 6.8 and the highest fluorescence emission was obtained at pH 7.4, which suggests that the formation of T-Hg^{2+}-T configuration was related to pH surroundings. Therefore, the solution pH value was maintained at 7.4 to obtain higher signal-to-noise ratio in the following experiments.

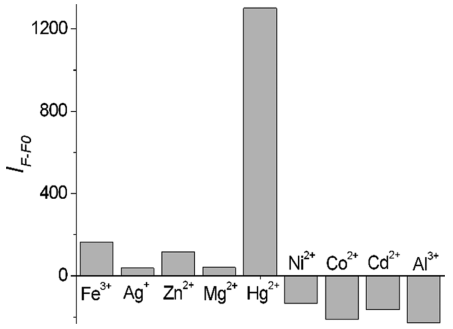

Figure 4. Specificity of the interaction between DNA aptamer and Hg^{2+} ions. Hg^{2+} ions were 3 μmol/L; Fe^{3+}, Ag^{+}, Zn^{2+}, Mg^{2+}, Ni^{2+}, Co^{2+}, Cd^{2+}, and Al^{3+} were all 3 mmol/L.

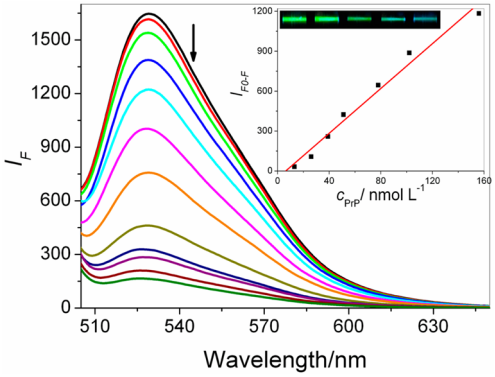

Figure 5. Label-free detection of $rPrP^{C}$ based on DNA aptamer and Hg^{2+} ions. The inset curve is the plot of fluorescence intensities measured at 529 nm vs the concentration of $rPrP^{C}$ ranging from 13.0 to156.0 nmol/L. The inset images were photographed excited at 490 nm, and the $rPrP^{C}$ concentrations ($\times 10^{-7}$ mol/L) from left to right were 0, 0.26, 0.78, 1.56, and 3.12, respectively. DNA aptamer, 10 nmol/L; Hg^{2+}, 3 μmol/L. All data were collected from three measurements, and the error bars indicate the standard deviation.

3.3. Mechanism of the Interaction between DNA Aptamer and Hg^{2+} Ions. To confirm the formation of double-strand structure induced by the specific and strong binding affinity of Hg^{2+} ions to T bases, we measured the circular dichroism spectra. As shown in Figure 3A, DNA aptamer alone has a negative peak nearby 250 nm and a positive peak around 270 nm, representing the characteristic

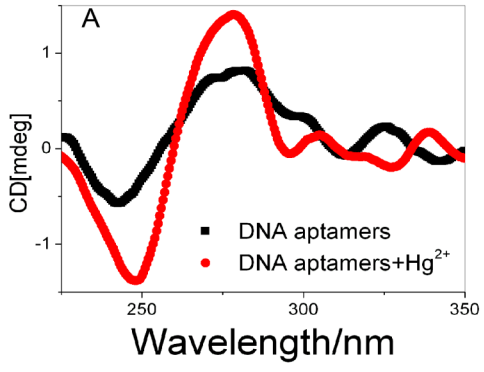

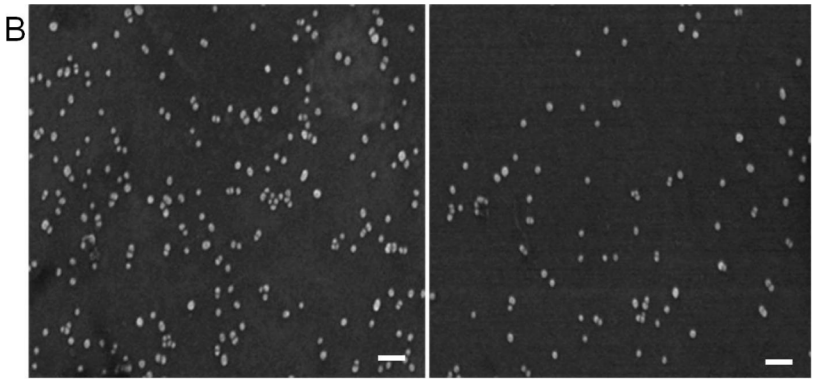

Figure 3. (A) Circular dichroism spectra of DNA aptamer with Hg^{2+}. 6×10^{-6} mol/L DNA aptamer was incubated with 0.3 mmol/L Hg^{2+} ions in the presence of 20 mmol/L PB buffer (pH 7.4) and 0.2 mol/L NaCl. (B) SEM images of Au NPs-Apt (left) and Au NPs-Apt incubating with 3 μmol/L Hg^{2+} (right) in the presence of 20 mmol/L PB buffer (pH 7.4) and 0.2 mol/L NaCl. Scale bars = 100 nm.

dx.doi.org/10.1021/jp302522b | J. Phys. Chem. B 2012, 116, 9565–9569

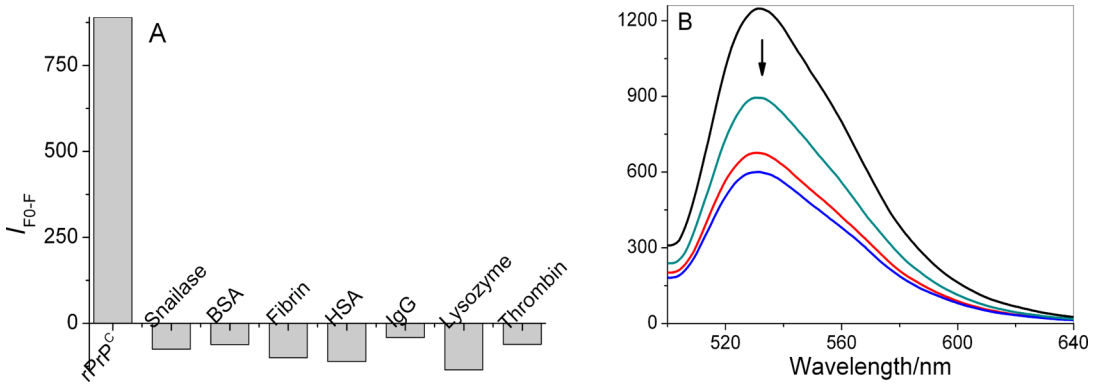

Figure 6. Specificity of the interaction between DNA aptamer-Hg^{2+} and $rPrP^C$. (A) Influences of other proteins. DNA aptamer, 10 nmol/L; Hg^{2+} ions, 3 μmol/L; $rPrP^C$, 1.02×10^{-7} mol/L (~3.9 μg/mL); snailase, BSA, fibrin, HSA, IgG, lysozyme, and thrombin were all 25 μg/mL. (B) Interaction between PrP^{Res} and DNA aptamer–Hg^{2+} complexes. PrP^{Res} concentrations from top to bottom are 0.0, 1.1, 2.2, and 3.3×10^{-7} mol/L; DNA aptamer, 10 nmol/L; Hg^{2+}, 3 μmol/L.

spectrum of single-strand DNA.[26] However, with the addition of Hg^{2+} ions, dramatic enhancement of the negative and positive peaks near 250 and 270 nm was observed, indicating an increase in DNA helicity and further suggesting the formation of double-strand structures.[26] To further verify that the double-strand structures formed inter- or intra-DNA aptamers, Au nanoparticles (Au NPs) were employed and the aggregation features of DNA-aptamer-modified Au NPs was measured.[23,27] Theoretically, if the T-Hg^{2+}-T configuration formed an intra-DNA aptamer, the Au NPs get aggregated, while the Au NPs remain dispersed in solution if the T-Hg^{2+}-T configuration formed inter-DNA aptamers. By modifying the DNA aptamer with Au NPs through thiol–gold covalent bonding, we prepared Au NPs-Apt conjugates first and measured their SEM images. As illustrated in Figure 3B, Au NPs were well dispersed even if incubated with 3 μmol/L Hg^{2+} ions, identifying the fact that the double-stranded structure was formed by inter-DNA aptamers through the specific interaction between T-rich DNA aptamer and Hg^{2+} ions, which results in dramatic fluorescence enhancement of Syber Green I.

With the purpose of illustrating the role of Hg^{2+} ions, the interactions between DNA aptamer and other metal ions rather than Hg^{2+} ions, such as Fe^{3+}, Ag^{+}, Zn^{2+}, Mg^{2+}, Ni^{2+}, Co^{2+}, Cd^{2+}, and Al^{3+}, were also measured. The results showed that other metal ions with the concentration 1000-fold higher than that of Hg^{2+} ions could not increase the fluorescence of Syber Green I (Figure 3), indicating that Hg^{2+} ions play a very important role in the formation of the double-stranded structure of DNA aptamer and that other metal ions that coexisted will not interfere in the interaction between DNA aptamer and Hg^{2+} ions.

3.4. Detection of $rPrP^C$. As the mechanism of the interaction between DNA aptamer and Hg^{2+} ions has been well demonstrated, we applied the DNA aptamer–Hg^{2+} complexes for the detection of $rPrP^C$. The results are shown in Figure 4. High fluorescence emission can be observed in the aqueous DNA aptamer–Hg^{2+} complexes; however, the fluorescence emission of Syber Green I decreased gradually with the addition of $rPrP^C$, indicating that double-strand structures formed by inter-DNA aptamers are destroyed owing to the specific and strong interaction between $rPrP^C$ and its DNA aptamer. Under the optimal condition, the decreased fluorescence intensities followed a linear relationship, which could be expressed as $\Delta I_F = 58.33 - 8.42 \times c_{rPrP}{}^C$ in the range of 13.0–156.0 nmol/L with the correlation coefficients of $R = 0.992$.

3.5. Specificity Study. For the specificity study, fluorescence changes brought by other proteins, such as snailase, BSA, fibrin, HSA, IgG, lysozyme, and thrombin, were compared with that brought by $rPrP^C$. The experimental results indicated that only $rPrP^C$ with the concentration of 1.02×10^{-7} mol/L (~3.9 μg/mL) caused a dramatic decrease in fluorescence. Other proteins, even if the concentrations were 6-fold higher than that of $rPrP^C$, could not cause a significant decrease in fluorescence (Figure 5), indicating that other proteins could neither interact with DNA aptamer–Hg^{2+} complexes nor destroy the T-Hg^{2+}-T configuration and the interaction between $rPrP^C$ and DNA aptamer was selective due to the inherent specificity of the DNA aptamer toward $rPrP^C$.

More significantly, we further investigated the interaction between DNA aptamer–Hg^{2+} complexes and diseases-associated isoform, PrP^{Res}, which was converted from $rPrP^C$ in vitro according to ref 25. The fluorescence of DNA aptamer–Hg^{2+} complexes was high in the absence of PrP^{Res} (Figure 6B, black line) while the fluorescence emission decreased gradually with increasing concentration of PrP^{Res}, suggesting that the double-strand structures formed by inter-DNA aptamer were destroyed by the specific interaction between PrP^{Res} and DNA aptamer. Since both PrP^C and PrP^{Res} can interact with the T-rich DNA aptamer, pretreatment like proteinase K digestion is needed to remove PrP^C in clinical diagnosis.

4. CONCLUSION

In summary, double-strand structures were formed by inter-DNA aptamers with the formation of T-Hg^{2+}-T configurations based on the specific binding affinity of Hg^{2+} to T-rich DNA aptamer, leading to significant fluorescence enhancement of double-strand specific dye Syber Green I. In the presence of target protein, $rPrP^C$, however, the specific and strong binding of $rPrP^C$ with DNA aptamer forced the destruction of double-strand structures formed by inter-DNA aptamers. As a consequence, the fluorescence emission of Syber Green I significantly decreased with increasing concentration of $rPrP^C$. All the results shown in this contribution demonstrate that the newly developed method based on DNA aptamer and Hg^{2+} possesses the great advantages of being label-free, easily

dx.doi.org/10.1021/jp302522b | J. Phys. Chem. B 2012, 116, 9565–9569

operated, cost-saving, sensitive, and specific, showing great promise for clinical detection.

AUTHOR INFORMATION

Corresponding Author

*E-mail: chengzhi@swu.edu.cn. Fax: (+86) 23 68866796. Tel.: (+86) 23 68254659.

Notes

The authors declare no competing financial interest.

ACKNOWLEDGMENTS

This research has been supported by the Ministry of Science and Technology of the People's Republic of China (No. 2011CB933600) and the Postgraduate Science and Technology Innovation Program of Southwest China University (No. ky2009004).

REFERENCES

(1) Soto, C. *Nat. Rev.* **2004**, *2*, 809.
(2) Grassi, J.; Maillet, S.; Simon, S.; Morel, N. *Vet. Res.* **2008**, *39*, 33.
(3) Lee, W.; Obubuafo, A.; Lee, Y.-I.; Davis, L. M.; Soper, S. A. *J. Fluoresc.* **2010**, *20*, 203.
(4) Zhang, J.; Wang, L.; Zhang, H.; Boey, F.; Song, S.; Fan, C. *Small* **2010**, *6*, 201.
(5) Liu, Y.; Tuleouva, N.; Ramanculov, E.; Revzin, A. *Anal. Chem.* **2010**, *82*, 8131.
(6) Yan, S.; Huang, R.; Zhou, Y.; Zhang, M.; Deng, M.; Wang, X.; Weng, X.; Zhou, X. *Chem. Commun.* **2011**, *47*, 1273.
(7) Phillips, J. A.; Lopez-Colon, D.; Zhu, Z.; Xu, Y.; Tan, W. *Anal. Chim. Acta* **2008**, *621*, 101.
(8) Goulko, A. A.; Li, F.; Le, X. C. *Trends Anal. Chem.* **2009**, *28*, 878.
(9) Li, C.; Lin, J.; Guo, Y.; Zhang, S. *Chem. Commun.* **2011**, *47*, 4442.
(10) Chen, L. Q.; Xiao, S. J.; Peng, L.; Wu, T.; Ling, J.; Li, Y. F.; Huang, C. Z. *J. Phys. Chem. B* **2010**, *114*, 3655.
(11) Martin, J. A.; Phillips, J. A.; Parekh, P.; Sefah, K.; Tan, W. *Mol. BioSyst.* **2011**, *7*, 1720.
(12) Cui, Z.-Q.; Ren, Q.; Wei, H.-P.; Chen, Z.; Deng, J.-Y.; Zhang, Z.-P.; Zhang, X.-E. *Nanoscale* **2011**, *3*, 2454.
(13) Gilch, S.; Schätzl, H. M. *Cell. Mol. Life Sci.* **2009**, *66*, 2445.
(14) Weiss, S.; Proske, D.; Neumann, M.; Groschup, M. H.; Kretzschmar, H. A.; Famulok, M.; Winnacker, E.-L. *J. Virol.* **1997**, *71*, 8790.
(15) Rhie, A.; Kirby, L.; Sayer, N.; Wellesley, R.; Disterer, P.; Sylvester, I.; Gill, A.; Hope, J.; James, W.; Tahiri-Alaoui, A. *J. Biol. Chem.* **2003**, *278*, 39697.
(16) Takemura, K.; Wang, P.; Vorberg, I.; Surewicz, W.; Priola, S. A.; Kanthasamy, A.; Pottathil, R.; Chen, S. G.; Sreevatsan, S. *Exp. Biol. Med.* **2006**, *231*, 204.
(17) Ogasawara, D.; Hasegawa, H.; Kaneko, K.; Sode, K.; Ikebukuro, K. *Prion* **2007**, *1*, 248.
(18) Bibby, D. F.; Gill, A. C.; Kirby, L.; Farquhar, C. F.; Bruce, M. E.; Garson, J. A. *J. Virol. Methods* **2008**, *151*, 107.
(19) Xiao, S. J.; Hu, P. P.; Wu, X. D.; Zou, Y. L.; Chen, L. Q.; Peng, L.; Ling, J.; Zhen, S. J.; Zhan, L.; Li, Y. F.; Huang, C. Z. *Anal. Chem.* **2010**, *82*, 9736.
(20) Ye, B.-C.; Yin, B.-C. *Angew. Chem., Int. Ed.* **2008**, *47*, 8386.
(21) Lee, J.; Jun, H.; Kim, J. *Adv. Mater.* **2009**, *21*, 3674.
(22) Wang, Y.; Li, J.; Jin, J.; Wang, H.; Tang, H.; Yang, R.; Wang, K. *Anal. Chem.* **2009**, *81*, 9703.
(23) Wang, Y.; Li, Y. F.; Wang, J.; Sang, Y.; Huang, C. Z. *Chem. Commun.* **2010**, *46*, 1332.
(24) Yu, S.-L.; Lei, J.; SY, M.-S.; Mei, F.-H.; Kang, S.-L.; Sun, G.-H.; Tien, P.; Wang, F.-S.; Xiao, G.-F. *Eur. J. Hum. Genet.* **2004**, *12*, 867.
(25) Bocharova, O. V.; Breydo, L.; Parfenov, A. S.; Salnikov, V. V.; Baskakov, I. V. *J. Mol. Biol.* **2005**, *346*, 645.
(26) Xiao, S. J.; Hu, P. P.; Li, Y. F.; Huang, C. Z.; Huang, T.; Xiao, G.-F. *Talanta* **2009**, *79*, 1283.
(27) Lee, J.-S.; Ulmann, P. A.; Han, M. S.; Mirkin, C. A. *Nano Lett.* **2008**, *8*, 529.